Author/s:
Imran, S;Neeland, MR;Peng, S;Vlahos, A;Martino, D;Dharmage, SC;Tang, MLK;Sawyer, S;Dang, TD;McWilliam, V;Peters, RL;Koplin, JJ;Perrett, KP;Novakovic, B;Saffery, R

Title:
Immuno-epigenomic analysis identifies attenuated interferon responses in naïve CD4 T cells of adolescents with peanut and multi-food allergy

Date:
2022-11-01

Citation:
Imran, S., Neeland, M. R., Peng, S., Vlahos, A., Martino, D., Dharmage, S. C., Tang, M. L. K., Sawyer, S., Dang, T. D., McWilliam, V., Peters, R. L., Koplin, J. J., Perrett, K. P., Novakovic, B. & Saffery, R. (2022). Immuno-epigenomic analysis identifies attenuated interferon responses in naïve CD4 T cells of adolescents with peanut and multi-food allergy. Pediatric Allergy and Immunology, 33 (11), https://doi.org/10.1111/pai.13890.

Imran Samira (Orcid ID: 0000-0002-8717-5502)
Martino David (Orcid ID: 0000-0001-6823-4696)
Dharmage Shyamali C (Orcid ID: 0000-0001-6063-1937)
Dang Thanh D (Orcid ID: 0000-0003-2010-5582)
Mc William Vicki (Orcid ID: 0000-0002-5000-2181)
Peters Rachel Louise (Orcid ID: 0000-0002-2411-6628)

Immuno-epigenomic analysis identifies attenuated interferon responses in naïve CD4 T cells of adolescents with peanut and multi-food allergy

Samira Imran[1], Melanie R Neeland[1], Stephen Peng, Amanda Vlahos[1], David Martino[1,2], Shyamali C Dharmage[1,4], Mimi LK Tang[1,3], Susan Sawyer[1,5], Thanh Dang[1], Vicki McWilliam[1,3], Rachel L Peters[1], Jennifer J Koplin[1], Kirsten P Perrett[1,3], Boris Novakovic[1*], Richard Saffery[1*]

[1]Murdoch Children's Research Institute, and Department of Paediatrics, University of Melbourne, Royal Children's Hospital, Flemington Road, Parkville, Victoria 3052, Australia

[2]Telethon Kids Institute, University of Western Australia.

[3]Department of Allergy and Immunology, Royal Children's Hospital, Melbourne, Victoria 3052, Australia

[4]Allergy and Lung Health Unit, Melbourne School of Population and Global Health, University of Melbourne

[5] Centre for Adolescent Health, Royal Children's Hospital Melbourne, Melbourne, Australia

*joint senior and corresponding authors: richard.saffery@mcri.edu.au and boris.novakovic@mcri.edu.au

Word count: 5,021 words

This is the author manuscript accepted for publication and has undergone full peer review but has not been through the copyediting, typesetting, pagination and proofreading process, which may lead to differences between this version and the Version of Record. Please cite this article as doi: 10.1111/pai.13890

Abstract

Background

IgE-mediated food allergies have been linked to suboptimal naïve CD4 T (nCD4T) cell activation in infancy, underlined by epigenetic and transcriptomic variation. Similar attenuated nCD4T cell activation in adolescents with food allergy have also been reported, but these are yet to be linked to specific epigenetic or transcriptional changes.

Methods

We generated genome-wide DNA methylation data in purified nCD4 T cells at quiescence and following activation in a cohort of adolescents (aged 10-15 years old) with peanut allergy (peanut only or peanut + ≥1 additional food allergy) (FA, n=29), and age-matched non-food allergic controls (NA, n=18). Additionally, we assessed transcriptome-wide gene expression and cytokine production in these cells following activation.

Results

We found widespread changes in DNA methylation in both NA and FA nCD4T cells in response to activation, associated with the T cell receptor signalling pathway. Adolescents with FA exhibit unique DNA methylation signatures at quiescence and post-activation at key genes involved in Th1/Th2 differentiation (*RUNX3, RXRA, NFKB1A, IL4R)*, including a differentially methylated region (DMR) at the *TNFRSF6B* promoter, linked to Th1 proliferation. Combined analysis of DNA methylation, transcriptomic data and cytokine output in the same samples identified an attenuated interferon response in nCD4T cells from FA individuals following activation, with decreased expression of several interferon genes, including IFN-γ and a DMR at a key downstream gene, *BST2*.

Conclusion

We find that attenuated nCD4T cell responses from adolescents with food allergy are associated with specific epigenetic variation, including disruption of interferon responses, indicating dysregulation of key immune pathways that may contribute to a persistent FA phenotype. However, we recognise the small sample size, and the consequent restraint on reporting adjusted P-value statistics as limitations of the study. Further study is required to validate these findings.

Keywords: nCD4T cells; adolescents; food allergy; peanut allergy; multi-food allergy; epigenetics; transcriptomics; interferon responses

Key Messages

We find that attenuated nCD4T cell responses from adolescents with food allergy are associated with specific epigenetic variation, including disruption of interferon responses, indicating dysregulation of key immune pathways that may contribute to a persistent FA phenotype.

Introduction

IgE-mediated food allergies (FA) are a major public health burden in developed countries, with limited treatment options. Current data indicate multi-factorial origins, with a number of environmental, genetic, and epigenetic variations underpinning FA-associated immune dysregulation, that impedes the development of oral tolerance to common allergens in early life[1-8]. While some food allergies (egg and milk) resolve within the first few years of life, adolescents with peanut allergy are less likely to acquire natural tolerance and are at higher risk of severe allergic reactions[9-12]. Peanut allergy tends to persist into adolescence and adulthood, often in conjunction with allergies to other foods such as tree nuts[12]. Adolescents with peanut allergy represent one of the highest risk groups for severe allergic reactions and poor quality of life[13-16].

A number of pathological immune responses in children with FA have been described[17-23]. These include differences in proportions of circulating innate and adaptive immune cell populations across egg and peanut allergy[17, 19, 21, 22]. Immune cells from egg-allergic infants show differential responses to activation relative to controls, with monocytes producing increased concentrations of proinflammatory cytokines (TNF-α, IL-6, MIP-1α) following stimulation with bacterial lipopolysaccharide. Naive CD4T cells from infants with egg allergy exhibit diminished lymphoproliferative responses following non-specific activation with anti-CD3 and anti-CD28, reflected at the molecular level by impaired expression of T cell activation genes, and epigenetic remodelling at genes linked to key metabolic pathways (*RPTOR, PIK3D, MAPK1 and FOXO1*) [17, 18, 24]. This attenuated T cell response is also evident in adolescents with FA, with nCD4 T cells producing significantly less IL-6, IL-8 and IFN-γ relative to healthy controls [21].

To determine the epigenetic basis for this altered naive CD4 T cell response in adolescents with food allergy, we generated genome-wide DNA methylation and RNA transcription profiles of quiescent and activated naïve CD4 T cells from adolescents (aged 10-15 years old) with peanut/multi-food allergy and age matched non-food allergic controls.

Methods

Clinical samples and data collection

This study was carried out using PBMC samples from a subset of adolescents enrolled in the SchoolNuts study, a cross-sectional population-based study profiling the prevalence of food allergy in adolescents aged between 10 and 15 years old. Food allergy was suspected based on parent-report and if the history suggested IgE-mediated food allergy, it was confirmed using skin prick tests and oral food challenges (OFC). If patient data indicated clear and recent history of adverse allergic reactions along with evidence of IgE-sensitization, OFCs were not required. Blood collections were carried out following patient visits. Food allergy was defined as a positive OFC or convincing recent or severe history in the context of IgE sensitisation (skin prick test (SPT) wheal size of ≥3mm or sIgE ≥0.35KuA/L), as described for the study previously[12]. Non-food allergic adolescents had no evidence of sensitisation (<3mm) to a panel of 15 food allergens by SPT (egg white, cow's milk, soy, peanut, cashew, almond, hazelnut, walnut, pistachio, macadamia, pecan, brazil nut, pine nut, sesame, shellfish). Additionally, the non-food allergic individuals had a history of tolerating the food. Peanut allergic adolescents (with or without concurrent sensitisations) were selected for the current study, along with non-food allergic controls

Ethics and consent

Ethics approval was obtained from the Royal Children's Hospital Human Research Ethics Committee (Human Research Ethics Committee no. 31079), the Department of Education and Early Childhood (Victorian Government, Australia), and the Catholic Education Office. Written informed consent was obtained from all participants.

Study participants

This study used samples from 47 adolescents from the SchoolNuts study: 18 age-matched non-food allergic controls (7 females, 11 males); and 29 food allergic adolescents (12 females and 17 males). In the food allergic group, 14 (5 females, 9 males) adolescents were allergic to only peanut, while 15 (7 females, 8 males) adolescents were allergic to peanut and at least one additional food. The food allergic and adolescents without food allergy were similar in regard to asthma and hay fever prevalence (Table 1).

Isolation of total nCD4T cell populations, culture and nucleic acid extraction

Isolation of nCD4T cell populations via flow cytometry

Peripheral blood mononuclear cells (PBMCs) were isolated from blood samples using Ficoll-Paque density gradient centrifugation as previously described, and cryopreserved in liquid nitrogen[18]. PBMCs were viably thawed and total nCD4T cell populations ($CD3^+CD4^+CD45RA^+$ $CCR7^+$) were isolated using fluorescence activated cell sorting (BD FACS-ARIA Fusion cell sorter). This protocol produced >95% pure nCD4T cell populations.

Culture

As outlined in a previous study, naïve CD4 T cells were resuspended at 8×10^4/200 µl in T-cell activation media (RPMI supplemented with 10% FCS, penicillin streptomycin and 200 IU/ml of IL2) and seeded (8×10^4/well) for 72 h at 37°C, 5% CO_2 [21]. At least 1.6×10^5 cells (two wells) were left unstimulated (cultured in RPMI alone; quiescent samples), while another 1.6×10^5 cells were stimulated with anti-CD3/CD28 T-cell activator Dynabeads (activated samples). Following this 72h incubation, replicate wells were pooled into Eppendorfs and centrifuged to obtain cell pellets. The supernatants were aspirated and stored separately for cytokine analysis, and cell pellets were resuspended in 350µl of RLT+2ME (QIAGEN) and stored at -80°C until future DNA and RNA extractions.

Isolation of nucleic acids

DNA and RNA were extracted from the quiescent and activated nCD4T cells using the QIAGEN AllPrep DNA/RNA micro-kit, according to manufacturers' protocols. DNA and RNA were quantified on the Qubit fluorometer using the Qubit dsDNA High Sensitivity (HS) Assay Kit, and the Qubit RNA HS assay kit (Thermofisher Scientific) respectively. RNA concentrations from quiescent samples did not reach thresholds for minimum starting input for next generation sequencing.

DNA methylation profiling

Genomic DNA from 47 paired activated and quiescent samples (200-500 ng) were randomised in a 96 well plate and sent to HuGe-F (Erasmus MC, Rotterdam, Netherlands) for bisulfite treatment and genome-wide methylation analysis using Illumina InfiniumMethylationEPIC BeadChips (the EPIC array), which detects methylation at over 850,000 CpG sites (EPIC probes) spanning gene bodies, promoters, regulatory elements (ENCODE open chromatin and enhancers)[25].

Raw data were received as .iDAT files, which were pre-processed using the minfi and MissMethyl packages (available from Bioconductor) in the R statistical environment[26, 27]. Assessment of sample quality revealed that 3/94 samples had a mean detection *P* value >0.01, thereby leaving 91 samples for analysis. An additional three samples (all from the quiescent NA group) were identified as outliers skewing the analysis and therefore removed from further analysis. The SWAN (Subset-quantile Within Array Normalization) approach was used to normalise data for technical variation between and within arrays[28]. Probes were then filtered to remove those with poor average quality scores *(P* value >0.01), cross-reactive probes and probes associated with single nucleotide polymorphisms (SNPs)[25]. Samples were run on two separate batches. In order to account for this, all probes affected by batch were identified using removed using the RUVfit approach.

The final dataset for analysis was comprised of methylation data from 712,879 probes in 88 samples. Confounders and covariates were identified using a principal component (PC) analysis (**Supplementary Figure 1**). Using available cohort data, covariates (traits) with complete data for all adolescents were as follows: age, sex, hayfever, wheeze, parent country of birth (within Australia/overseas), sample position on the EPIC array (batch, plate well and position on chip); DNA concentration (ng/µl) and DNA volume (µl). Traits that significantly contributed to one of the first 5 PCs (R^2 >0.2, p <0.05) were incorporated into the model for differential analysis. The final statistical model was: 'food allergy group + sex + batch + plate well + position on chip +DNA amount + DNA concentration + parent country of birth + batch + individual). Differential analysis was carried out on the 712,879 probes using a linear regression model with limma[29]. Differentially methylated probes in the quiescent vs activated comparisons were identified as those showing an adjusted *P* value <0.01 and a methylation difference ($\Delta\beta$) >5%; while DMPs from the NA vs FA comparisons defined as those showing an unadjusted *P* value <0.01 and $\Delta\beta$ >5%. The DMRCate tool was used to determine differentially methylated regions (DMRs), and individual probes within these DMRs were identified using Bedtools[30, 31]. Significant DMRs were identified as those showing a *P* value <0.05, and consisting of 4 or more probes, with at least one probe showing a $\Delta\beta$ >5%. The nearest genes (within 1Mb of transcription start site in any one direction) to these DMRs and DMPs were determined using the web-based GREAT tool[32]. Functional enrichment analysis on genes associated with these probes was carried out using the GoMeth feature of the MissMethyl package on R. DNA methylation data are available on the GEO repository, accession code GSE189148.

Transcriptomic profiling

Isolated RNA from 47 paired stimulated nCD4T samples was sent for next generation sequencing on the Illumina NovaSeq 6000 instrument to the Translational Genomics Unit at the Victorian Clinical Genetics Services. Libraries were prepared using the Illumina TruSeq Stranded mRNA Kit with a starting input of 100 ng (where available) and subsequently sequenced; with the generation of approximately 20 million reads per sample, 100bp paired-end. Raw data were received as fastq files, which were subject to a quality check using FastQC, with all samples passing QC. Reads were then aligned to the human transcriptome (GrCh37 v70) using Bowtie2, and gene counts were derived using HTSEQ. Only protein-coding genes were selected for differential gene expression analysis, leaving expression data for 20,232 genes. Genes exhibiting low expression (mean reads per kilobase of transcript, per million of mapped reads (RPKM) <1 across all samples) were removed from analysis. The DESeq2 package (available on Bioconductor) was used to normalise count data and determine gene expression differences between group comparisons[33]. Differentially expressed genes were defined as those reaching $P < 0.05$, and showing a fold change > 1.5 between NA and FA samples. RNA-seq data are available on the GEO repository, accession code GSE189149.

Analysis of publicly available ATAC-seq data

Assay for Transposable Accessible Chromatin (ATAC)-seq fastq files for quiescent and activated T cells were downloaded from GEO (GSE157174)[34]. ATAC-seq reads were aligned to human genome assembly hg19 using bwa[35]. BAM files were first filtered to remove the reads with mapping quality less than 15 using samtools[36], and MACS2 was used to call peaks[37]. Peaks from all samples were merged into a single ATAC peaks .bed file and reads per peak were counted using bedtools[31]. For visualisation in the UCSC Genome Browser, bam file were converted into bigwig files using the bamCoverage tool in deepTools[38]. Data (reads/peak) were normalized using the R package DESeq2[39]. ATAC-seq reads/peak were overlapped with DMPs and DMRs from activated vs quiescent comparisons of NA and FA nCD4T cells; and comparisons of NA vs FA (at quiescence and post activation) using bedtools.

CD4 T cell subset deconvolution

In order to identify signatures of CD4 T cell subsets in the activated samples, we obtained scRNAseq data from a previously published study that identified T cell subset signatures post

activation[40]. This data was re-clustered on Seurat (v2.3.0) to identify cell populations of interest, and count data from selected populations were extracted and uploaded onto Cibersortx[41, 42]. A signature matrix was constructed from this data with default parameters adjusted to include data from 100 replicates, minimum expression threshold of 0.5 (as background data was derived from the droplet-based 10x Chromium platform) and 300-500 barcode genes per cell type. Bulk RNA-seq data (counts per million values) of protein coding genes (20, 032 genes) from our study was uploaded onto the server, and cell fractionation analysis was carried out with S-mode batch correction enabled and running 1000 permutations. Results of fractionation analysis were downloaded and scaled across samples.

Results

DNA methylation signature of nCD4T cell activation in food allergic adolescents

Purified naïve CD4 T cells from adolescents with food allergy (peanut allergy only, and peanut allergy + ≥1 additional food allergy; FA, n=29) and non-food allergic controls (NA, n=18) were cultured for 72 hours in media alone ('quiescent') or with anti-CD3/anti-CD28 beads ('activated') (**Figure 1A**), followed by DNA isolation and genome-wide DNA methylation profiling. A total of 7,676 differentially methylated probes (DMPs) were identified between stimulated and quiescent samples in the NA group and 10,503 DMPs in the FA group (adjusted *P* value < 0.01, and $\Delta\beta$ >5%; **Figure 1B, Supplementary Table 1**). Combined, there were 11,584 DMPs distinguishing quiescent and activated nCD4T cells across NA and FA adolescents.

Principal component analysis (PCA), based on the combined list of 11,584 DMPs, showed clear separation of samples by T-cell activation status (PCA1) but not allergic phenotype (**Figure 2A**). This is reflected in the number of common DMPs (n= 6,773) in both NA and FA groups (**Figure 2B).** Nevertheless, 1,081 DMPs were specific to NA (590 DMPs showing higher DNAme, 491 DMPs showing lower DNAme in activated samples); and 3,908 DMPs specific to FA (1080 DMPs showing higher DNAme, 2,828 DMPs showing lower DNAme in activated samples) following activation (**Figure 2B**). Similar enrichment terms were found when functional enrichment analysis was carried out on genes associated with these three sets of probes from the Venn diagram (NA specific, commonly activated, FA specific) (**Supplementary Figure 2**). Shared DMPs between NA and FA adolescents showed the strongest changes in DNA methylation following activation, while the NA-specific and FA-specific DMPs showed a more subtle difference, as indicated by boxplots of the methylation differences of these DMPs (**Supplementary Figure 1C**).

To determine the likelihood that changes in DNA methylation corresponded to changes in chromatin accessibility, we compared these activation-associated DMPs (commonly activated, NA-specific and FA-specific) to a publicly available ATAC-seq dataset for nCD4T cells at quiescence and following activation using the same approach (72 hours with anti-CD3/CD28)[34]. We identified enrichment for ATAC-peaks in commonly activated DMPs (33% relative to 21% for all EPIC probes; (X^2 (3, N = 11,584) = 82.7, *P* value <.01)) **(Supplementary Figure 2).** Generally speaking, DMPs showing a gain of methylation were associated with a decrease in chromatin accessibility and *vice versa*, indicating that the DNA

methylation changes induced by activation are likely accompanied by nucleosome repositioning and DNA accessibility (**Supplementary Figures 1 and 2**).

Differential methylation between FA and NA nCD4T cells at quiescence

Using an unadjusted *P* value cut-off <0.01 and $\Delta\beta$ >5% between groups, we found 347 DMPs at quiescence (247 showing showing higher DNAme, and 100 showing showing lower DNAme in FA) (**Figure 3A; Supplementary Table 3**). While this DMP signature clearly distinguished the NA and FA groups (**Figure 3B, 3C and 3D**) there was no enrichment for gene pathway terms, proximity to CpG islands or overlap with ATAC peaks in healthy nCD4T cell data from infants (**Supplementary Table 3, Supplementary Figure 3)**. Hierarchical clustering based on these 347 DMPs from the comparison of quiescent NA and FA nCD4T cells showed a clear separation of NA and FA samples at quiescence, but limited distinction between activated NA and activated FA samples (**Figure 3D**).

To further characterise the difference in NA and FA epigenomes at quiescence, DMRs were determined using DMRCate. We found 17 DMRs with unadjusted *P* value <0.05 (>3 probes in DMR, ≥1 probe $\Delta\beta$ greater than 5%) (**Supplementary Figure 3D, Supplementary Table 4)**. Of these, 14 DMRs showed higher methylation, while 3 DMRs showed lower methylation in FA. This included DMRs associated with genes previously linked to immune disorders and T cell activation, such as *GLI2* and *SLFN12*[43-46]. One of the DMRs showing higher methylation in the FA group ($\Delta\beta$ 1.5%-9.3%) is located in the promoter of *TNFRSF6B*. This gene has previously been linked to other inflammatory diseases such as multiple sclerosis, rheumatoid arthritis and psoriasis[47-53] (**Supplementary Figure 3E)**. This DMR consisted of 7 probes and was located in an accessible chromatin region based on nCD4 T cell ATAC-seq data from healthy infants[34].

Interestingly, we found increased enrichment (X^2 (3, N = 668) = 43.3, *P* value < .01) for open chromatin regions (based on healthy T cell data) among these DMRs, with 46% of DMRs associated with ATAC peaks in healthy nCD4 T cell data (**Supplementary Table 4, Supplementary Figure 3B**). These DMRs were located at CpG islands (22% of DMRs), and at shores of CpG islands (50% of DMRs) at a higher density compared to overall distribution of EPIC probes, indicating that these differences are occurring at regions of active transcription in T cells and therefore functionally relevant (**Supplementary Figure 3**).

Differential methylation between FA and NA nCD4T cells following activation

Next, we compared DNA methylation patterns between NA and FA groups following activation. Using an unadjusted *P* value threshold <0.01, we found 5,125 DMPs, of which 289 (151 probes showed showing higher DNAme and 138 showed showing lower DNAme in FA samples) at a $\Delta\beta$ >5% between groups (**Figure 1B and Figure 4A**).

Combining DMPs from both quiescent and activated comparisons, produced a total of 594 DMPs. Principal components analysis indicated that these probes clearly distinguished NA and FA samples (PC1), and quiescent from activated samples (PC2; **Figure 4B**). Hierarchical clustering based on the 289 DMPs from the activated comparison showed a very clear distinction of NA and FA samples at both quiescence and following activation (**Figure 4C**). Interestingly, functional enrichment analysis carried out on genes associated with NAvFA DMPs post activation reveals differential methylation at probes associated with the Th1 and Th2 differentiation pathway (**Figure 4D**). Probes located near *NFKB1* and *IL4R* showed showing lower DNAme in the FA group, while probes associated with *RUNX3* and *RXRA* showed showing higher DNAme in activated FA samples (**Figure 4E**).

We also assessed the distribution of DMRs relative to CpG islands between NA and FA samples following activation. Using similar criteria for differential methylation (*P* value <0.05, >3 probes in DMR, ≥1 probe $\Delta\beta$ greater than 5%) we found 15 DMRs, of which 8 showed higher, and 7 showed lower, methylation in FA relative to NA (**Supplementary Figure 4, Supplementary Table 5**). Of these DMRs, 53% were associated with an ATAC peak in healthy nCD4T cells, and 53% of DMRs were associated with CpG islands (**Supplementary Table 5, Supplementary Figure 3**). This highlights the likely functional relevance of these DMRs that distinguish NA and FA nCD4T cells following activation.

Activated CD4T cell subset deconvolution

In addition to methylation data, we generated transcriptomic data for activated nCD4T cell samples (**Figure 1A**). To determine whether there were variations in proportions of T cell subsets between NA and FA samples following activation that might account for some of the observed differential methylation, we compared bulk RNA-seq data from our study to previously published scRNA-seq data profiling expression of CD4 T cell subsets post

activation (**Figure 5A**) using the web-based tool CIBERSORTx[40, 42]. Based on these data, we found higher expression of induced regulatory T cell signatures in the FA adolescents following activation relative to controls, which reflected higher proportions of activated regulatory T cells in these adolescents, as reported in a previous study by our group[21]. Interestingly, we found that relative to NA adolescents, FA adolescents exhibited lower expression of IFN-producing cell signatures (**Figure 5B**). The signature genes for each of these cell types are outlined in the study that assessed these scRNA signatures[40]. Signature genes for the iTreg cell type included *LMCD1, FOXP3, DNAJC12, LGALS3, VIM, NELL2, SIRT1, PGM2L1, CCL5,* and *RGS1*. The signature gene set for the IFN-producing cell type consisted of 50 genes, which included several *OAS* genes, interferon-associated genes and genes involved in pathways such as GTPase activity and cell lysis (*MX1, GZMA*). We did not detect any differences between NA and FA adolescents for expression of Th0-, Th2- or Th17-associated signatures.

Differential methylation and expression of interferon-associated genes in FA nCD4T cells following activation

We also carried out differential gene expression analysis between activated samples from NA and FA adolescents. A total of 89 differentially expressed genes (DEGs) were identified across FA and NA adolescents post activation, (*P* value <0.05; foldchange >1.5), of which 46 genes showed lower, and 43 genes showed higher expression in FA samples (**Figures 5C**). Similar to DNA methylation data (**Supplementary Figure 4**), this gene expression signature separated the NA and FA groups as shown by both heatmap and PCA plots (**Figure 5C, D**). However, we observed minimal overlap between methylation signatures and gene expression signatures, with only 4/89 DEGs (*CXCR6, DTX1, RXRA* and *SLC9A3*) associated with a DMP within 1Mb of the gene TSS, but no genes were associated with a nearby DMR.

Gene ontology analysis of DEGs between NA and FA individuals revealed enrichment for a number of interferon response terms, such as type 1 interferon signalling pathway, (GO:0060337, FDR = 1.05e-17, genes in term: *IFIH1, IFITM3, RSAD2, OAS1, IFI44, CCL4, ISG20, DDX58, IFIT3, IFIT2, OASL, IFIT1, DDX60, IFNG* and *MX2*), negative regulation of type I interferon production (GO:0032480, FDR=0.08, genes in term = *DDX58, IFIH1, ISG15* and *HERC5*), and cellular response to interferon-alpha (GO:0035457, FDR= 0.32, genes in term= *IFIT3, IFIT2* and *OAS1*) (**Figure 5E and Figure 6A).**

Previous analysis of the same cohort showed reduced production of IL-6, TNF-α and IFN-γ cytokines post activation in nCD4 T cells from FA adolescents[21]. While we did not find any evidence of differences in IL-6 and TNF-α transcription in the current study, we observed lower expression of IFN-γ in FA adolescents (fold change = 3.25, *P* value < 0.01) (**Figure 6B)**.

We also found evidence of a DMR ($\Delta\beta$ 1.1%-6.7%; higher in FA) near the *BST2* gene promoter, an interferon stimulated gene, further suggesting that disruption of interferon pathways is associated with differential methylation in FA (**Figure 6C, D)**. This DMR spanned 886 base pairs and consisted of 12 probes, where 4 probes were significantly differentially methylated between NA and FA groups (*P* value <0.01, $\Delta\beta$ >5%) (**Figure 6C**). Moreover, this DMR occurs at an open chromatin region in nCD4 T cells, based on ATAC-seq data from healthy infants, indicating that differential methylation at this locus may directly impact gene expression (**Figure 6D**). While *BST2* was downregulated in the FA samples (*P* value <0.01), there was only a 1.3 fold change in expression between NA and FA samples, which did not reach the cutoff (foldchange > 1.5) applied for significant differences in gene expression (**Supplementary Figure 4**).

Discussion

Our group recently demonstrated altered cytokine responses (decreased production of IL-6, TNF-α and IFN-γ compared to NA controls) following activation of naïve CD4 T cells in adolescents with peanut allergy, however specific epigenetic or transcriptional changes underlying this deficit were not investigated [21]. In this study, we linked these altered responses to epigenetic variation in FA adolescents. While NA and FA individuals overall appear to respond similar responses to activation, we show specific differential methylation at a number of T cell differentiation genes (*IL4R, NFKB1A, RUNX3, RXRA)* between NA and FA adolescents, and report an extended genomic region showing higher methylation in FA near *TNFRSF6B*. Analysis of transcriptomic data from activated nCD4T cells shows lower production of several interferon-associated genes in the FA group, which was corroborated with previously published scRNAseq data and cytokine data to highlight the impaired interferon response in FA adolescents. This attenuated interferon response was also reflected in the epigenome, with FA adolescents showing higher methylation at the *BST2* promoter.

Naïve CD4 T cells from NA and FA adolescents respond similarly to activation

In this study we demonstrated that purified nCD4T cells from NA and FA adolescents show minimal differences in epigenomes in response to activation with significant overlap of activation-linked DMPs between NA and FA adolescents, and less than half of the probes from either comparison showing NA- or FA-specific responses. This contrasts with findings from a previous study by our group that used the same model of ex vivo nCD4T cell activation from egg-allergic infants and healthy controls, where we uncovered a signature of 558 CpG sites differentiating quiescent and activated nCD4 T cells, as well as NA and FA infants following activation[17]. This suggests that changes in the epigenome in association with T cell activation may vary by age and/or allergy type. Future studies profiling T cell responses across age may elucidate potential age-linked epigenomic differences.

Interestingly, probes showing NA-specific activation patterns exhibited the least consistency with the publicly available ATAC-seq data. This discrepancy may be caused by the age difference between the adolescent dataset and the ATAC-seq dataset (from infants), whereas FA-specific probes showed significant overlap with ATAC-seq signatures. This finding requires further analysis, preferably with an ATAC-seq dataset in adolescent T cells.

Epigenetic differences between NA and FA at quiescence

We identified potential differences between epigenomes of nCD4T cells from NA and FA adolescents at quiescence. One of these regions, showing higher methylation in the FA, was located in the promoter region of *TNFRSF6B*, a gene encoding the death decoy receptor 3 (DcR3), a member of the TNF receptor family. DcR3 functions as an immunomodulatory molecule involved in a number of immune mechanisms including T cell activation, as well as B cell activation and monocyte-dendritic cell differentiation[51, 54, 55], and has been linked to a number of diseases such as asthma, rheumatoid arthritis, multiple sclerosis, systemic lupus erythematosus, inflammatory bowel disease and psoriasis. In murine models, overexpression of DcR3 has been associated with impaired Th1 differentiation[52]. Accordingly, in rheumatoid arthritis and multiple sclerosis, increased levels of DcR3 are associated with decreased levels of IFN-γ and reduced T cell proliferation[55, 56]. However, DcR3 co-stimulation has been shown to enhance T cell proliferation in serum samples from patients with SLE, and increased expression of DcR3 was associated with enhanced disease activity[51]. Studies assessing DcR3 expression in relation to asthma and other atopic disorders expression showed increased levels of DcR3 in atopic individuals[53, 57]. Based on these studies, it is evident that DcR3 plays a key role in T cell activation and consequently IFN-γ expression, and differential methylation at this locus in FA adolescents at baseline may be indicative of an epigenome primed for differential responses following activation.

Epigenetic variation at T cell differentiation genes between activated samples from NA and FA adolescents

The minimal overlap between quiescent and activated DMPs suggests that the methylation overlap observed at quiescence are no longer apparent following activation, but also represents a new divergent methylation signature between NA and FA samples following activation. This suggests T cell activation unmasks unique methylation signatures in FA adolescents, with accentuated differences at probes associated with T cell differentiation genes (*IL4R, NFKB1, RXRA* and *RUNX3*). While the Th1/Th2 paradigm has become a hallmark of FA and it is well established that transition from naïve to Th1 or Th2 cells involves specific epigenetic variation and expression of key genes involved in T cell lineage specification, there are few studies directly implicating differences in DNA methylation in mediating this phenotype.

We have previously shown that nCD4T cells from egg-allergic infants show epigenetic reprogramming at genes encoding proinflammatory cytokines such as *IL1R, IL18RAP* and *CD28* . Other studies examining DNA methylation profiles of children (ages 5-17) with cow's

milk allergy have also shown higher methylation at Th1 genes (*IFN-γ* and *IL-10*) and lower methylation of Th2-related genes in PBMCs of children with active FA compared to those who had acquired tolerance[1]. More recently, a twin study (n=20, aged 5-10 years) looking at discordant peanut allergy in mono- and dizygotic twins revealed decreased methylation at *IL4*, and higher methylation at *IL2* and *IL12B* in PBMCs from children with peanut allergy[58]. Methylation differences at these loci have been associated with peanut allergy reaction severity[59]. However, to our knowledge, we are the first to report DNA methylation changes at these Th1/Th2/Th17 genes in naïve CD4 T cells from adolescents with FA in response to non-specific activation conditions.

Impaired interferon response in FA adolescents

The antagonistic roles of IFN-γ and IL-4 in Th1/Th2 differentiation play a fundamental role in atopic disorders, with FA adolescents typically exhibiting a skew towards IL-4, and diminished expression of IFN-γ[60-62]. In line with this, our data demonstrated a clear pattern of impaired interferon responses in the FA adolescents across transcriptomic, DNA methylation and cytokine profiles. In the transcriptomic data, we found decreased expression of a number of interferon-stimulated genes linked to the type 1 interferon pathway and diminished expression of IFN-γ in FA adolescents following activation, which complements the cytokines profiles of these adolescents outlined in a previous study by our group[21]. Moreover, nCD4T cell deconvolution analysis using transcriptome-wide expression data, compared to previously published CD4T cell scRNA data, reveals lower expression of IFN-producing cell signatures in the FA group indicating an aberrant response to activation in the FA adolescents.

We found a DMR showing higher methylation in FA samples located in the promoter of *BST2,* encoding bone stromal antigen 2, a marker of interferon producing cells in mice[63]. Furthermore, stimulation with type 1 interferons induces expression of *BST2* across various cell types[63]. Adolescents with SLE and psoriasis, diseases characterised by increased IFN-α activity, typically exhibit enhanced expression of *BST2* in PBMC samples[64, 65]. A drug consisting of component of BST-2 conjugated with IgG Fc has been shown to mediate airway inflammation in murine models of asthma[66]. This suggests that higher methylation at *BST2* in nCD4T cells of adolescents with FA may be an indication of altered type 1 interferon responses following activation.

The role of type 1 interferons in allergic disorders is becoming increasingly important, which inhibit Th2 differentiation by suppressing *GATA3* activity[67, 68]. However, this regulation takes

place at the level of histone modifications as opposed to DNA methylation, which may account for the relatively minimal changes observed at these genes in our data. It is possible that the DNA methylation differences we observed between NA and FA CD4 T cells are a downstream effect of other epigenetic mechanisms.

Strengths and limitations

Our study represents one of the few in the field to profile genome-wide epigenetic and transcriptional signatures in an isolated cell population in food allergy. Additionally, we are the first to apply a multi-omic analysis of T cell mediated immune responses in adolescents with food allergy.

However, we acknowledge the small sample size, the heterogeneity of our FA group (consisting of both single peanut and multi-food allergic adolescents), and the absence of gene expression data from the quiescent samples as limitations in our study. The small sample size may have contributed to the failure to detect probes reaching FDR significance in the group comparisons. Our study was exploratory in nature and although we were underpowered to detect genome-wide significant associations, we applied a threshold of un-adjusted P value < 0.01 and effect size +/- 5% to rank candidates and utilized publicly available data sets from other epigenetic markers to corroborate our findings. Our results therefore provide novel hypotheses to test in future studies with larger group sizes. Additionally, the data used to assess chromatin accessibility at probes and regions showing differential methylation were derived from a study looking at nCD4 T cells from non-food allergic infants, which may differ from chromatin landscapes of adolescents. We also note the variability in the ethnicity of the NA and FA adolescents (parents of 89% of NA adolescents were both born in Australia, compared to 66% of parents of FA adolescents); which may have contributed to epigenetic differences. However, the model for differential analysis incorporated ethnicity as a covariate to minimise potential variation. While the heterogeneous nature of the FA adolescents potentially promoted variability in the FA group, we view this heterogeneity as a strength of our study as it is an accurate representation of the FA demographic in this age group[9, 11, 12]. We recognise that gene expression data from the quiescent samples would have proven useful in characterising the profile of T cell transcriptional changes in NA and FA adolescents. However, the transcriptomic differences found following activation are sufficient in portraying the differential gene expression following activation in FA adolescents.

Conclusion

This exploratory study suggests potential epigenetic differences between NA and FA adolescents at both quiescence and following activation relating to genes previously linked to inflammatory diseases (*SLFN12, GLI2, TNFRSF6B*), and more pronounced divergent methylation signatures at genes linked to Th1/Th2 differentiation genes (*IL4R, RUNX3, RXRA, NFKB1A*) following activation. Moreover, transcriptomic data reveals extensive disruption of interferon signalling pathways in FA samples post-activation and these findings are supported by DNA methylation and cytokine profiles. However, we recognise the small sample size, and the consequent restraint on reporting adjusted P-value statistics as limitations of the study. Future studies must improve on these limitations and further assess changes at the level of histone modifications and a direct examination of CD4 T cell subset frequencies following activation re required to determine whether these DNA methylation changes translate into immunophenotypic differences.

Table 1: Table of demographics for subset of SchoolNuts cohort used in this study

	Non-food allergic (NA)	Food allergic (FA)
Total number	18	29
Sex: male, n (%)	11 (61%)	17 (59%)
Age at blood collection (years), median (min-max)	13 (10-15)	13 (11-14)
Current asthma/wheeze, n (%)	9 (50%)	14 (52%) [2 ND][a]
Hayfever , n (%)	12 (67%)	20 (71%) [1 ND]
Family history of food allergy, n (%)	7 (39%) [1 ND]	7 (25%) 1 [ND]
Both parents born in Australia, n (%)	16 (89%)	19 (66%)
Peanut SPT (mm), median (min-max)	0 (0-2)	10 (6-35) [1 ND]
Peanut sIgE (kUA/L), median (min-max)	0.2 (0.07-0.31)	4.64 (0.5-68 (67.5)) [4 ND]
Peanut Allergy + concurrent sensitisation[b]	0 (0%)	15 (52%)

[a]Not defined

[b]Allergy to one or more of the following foods: tree nuts (either cashew, pistachio, walnut, hazelnut, macadamia, pecan, almond, Brazil nut or pine nut), sesame, egg, milk or shellfish.

Conflict of interest

The authors declare no conflicts of interest.

Acknowledgments

This study was funded by an NHMRC (Australia) Project Grant (#1165073) to RS, MN and BN. The SchoolNuts study was funded by an NHMRC Project Grant (#1047396). BN is supported by an NHMRC (Australia) Investigator Grant (#1173314). MN is supported by a Melbourne Children's LifeCourse Fellowship. KP is supported by a Melbourne Children's Clinician Scientist Fellowship. JK is supported by an NHMRC (Australia) Investigator Grant (#1158699).We thank the students, parents, and schools that participated in the SchoolNuts study.

References

1. Berni Canani R, Paparo L, Nocerino R, *et al.* Differences in DNA methylation profile of Th1 and Th2 cytokine genes are associated with tolerance acquisition in children with IgE-mediated cow's milk allergy. *Clin Epigenetics* 2015; **7**: 38.
2. Chang C, Wu H, Lu Q. The Epigenetics of Food Allergy. *Adv Exp Med Biol* 2020; **1253**: 141-152.
3. Hong X, Wang X. Epigenetics and development of food allergy (FA) in early childhood. *Curr Allergy Asthma Rep* 2014; **14**: 460.
4. Krajewski D, Kaczenski E, Rovatti J, *et al.* Epigenetic Regulation via Altered Histone Acetylation Results in Suppression of Mast Cell Function and Mast Cell-Mediated Food Allergic Responses. *Front Immunol* 2018; **9**: 2414.
5. Martino D, Dang T, Sexton-Oates A, *et al.* Blood DNA methylation biomarkers predict clinical reactivity in food-sensitized infants. *J Allergy Clin Immunol* 2015; **135**: 1319-1328.e1311-1312.
6. Martino D, Joo JE, Sexton-Oates A, *et al.* Epigenome-wide association study reveals longitudinally stable DNA methylation differences in CD4+ T cells from children with IgE-mediated food allergy. *Epigenetics* 2014; **9**: 998-1006.
7. Paparo L, Nocerino R, Cosenza L, *et al.* Epigenetic features of FoxP3 in children with cow's milk allergy. *Clin Epigenetics* 2016; **8**: 86.
8. Peng C, Van Meel ER, Cardenas A, *et al.* Epigenome-wide association study reveals methylation pathways associated with childhood allergic sensitization. *Epigenetics* 2019; **14**: 445-466.
9. McWilliam V, Koplin J, Lodge C, Tang M, Dharmage S, Allen K. The Prevalence of Tree Nut Allergy: A Systematic Review. *Curr Allergy Asthma Rep* 2015; **15**: 54.
10. McWilliam V, Peters R, Tang MLK, *et al.* Patterns of tree nut sensitization and allergy in the first 6 years of life in a population-based cohort. *J Allergy Clin Immunol* 2019; **143**: 644-650.e645.
11. McWilliam VL, Perrett KP, Dang T, Peters RL. Prevalence and natural history of tree nut allergy. *Annals of allergy, asthma & immunology : official publication of the American College of Allergy, Asthma, & Immunology* 2020.
12. Sasaki M, Koplin JJ, Dharmage SC, *et al.* Prevalence of clinic-defined food allergy in early adolescence: The SchoolNuts study. *Journal of Allergy and Clinical Immunology* 2018; **141**: 391-398.e394.
13. Doyle AJ. Anaphylactic reactions to peanuts. *Br Dent J* 1995; **178**: 87-88.
14. Hourihane JO. Peanut allergy--current status and future challenges. *Clin Exp Allergy* 1997; **27**: 1240-1246.
15. Loza C, Brostoff J. Peanut allergy. *Clin Exp Allergy* 1995; **25**: 493-502.
16. Sicherer SH, Sampson HA. Food allergy: A review and update on epidemiology, pathogenesis, diagnosis, prevention, and management. *Journal of Allergy and Clinical Immunology* 2018; **141**: 41-58.
17. Martino D, Neeland M, Dang T, *et al.* Epigenetic dysregulation of naive CD4+ T-cell activation genes in childhood food allergy. *Nat Commun* 2018; **9**: 3308.
18. Neeland MR, Koplin JJ, Dang TD, *et al.* Early life innate immune signatures of persistent food allergy. *J Allergy Clin Immunol* 2018; **142**: 857-864.e853.
19. Neeland MR, Martino DJ, Dang TD, *et al.* B-cell phenotype and function in infants with egg allergy. *Allergy* 2019; **74**: 1022-1025.
20. Weissler KA, Rasooly M, DiMaggio T, *et al.* Identification and analysis of peanut-specific effector T and regulatory T cells in children allergic and tolerant to peanut. *J Allergy Clin Immunol* 2018; **141**: 1699-1710.e1697.

21. Neeland MR, Andorf S, Dang TD, *et al.* Altered immune cell profiles and impaired CD4 T-cell activation in single and multi-food allergic adolescents. *Clin Exp Allergy* 2021; **51**: 674-684.
22. Neeland MR, Andorf S, Manohar M, *et al.* Mass cytometry reveals cellular fingerprint associated with IgE+ peanut tolerance and allergy in early life. *Nature Communications* 2020; **11**: 1091.
23. Zhang Y, Collier F, Naselli G, *et al.* Cord blood monocyte-derived inflammatory cytokines suppress IL-2 and induce nonclassic "T(H)2-type" immunity associated with development of food allergy. *Sci Transl Med* 2016; **8**: 321ra328.
24. Martino DJ, Bosco A, McKenna KL, *et al.* T-cell activation genes differentially expressed at birth in CD4+ T-cells from children who develop IgE food allergy. *Allergy* 2012; **67**: 191-200.
25. Pidsley R, Zotenko E, Peters TJ, *et al.* Critical evaluation of the Illumina MethylationEPIC BeadChip microarray for whole-genome DNA methylation profiling. *Genome Biol* 2016; **17**: 208-208.
26. Fortin J-P, Triche TJ, Jr, Hansen KD. Preprocessing, normalization and integration of the Illumina HumanMethylationEPIC array with minfi. *Bioinformatics* 2016; **33**: 558-560.
27. Phipson B, Maksimovic J, Oshlack A. missMethyl: an R package for analyzing data from Illumina's HumanMethylation450 platform. *Bioinformatics* 2016; **32**: 286-288.
28. Maksimovic J, Gordon L, Oshlack A. SWAN: Subset-quantile within array normalization for illumina infinium HumanMethylation450 BeadChips. *Genome Biol* 2012; **13**: R44.
29. Ritchie ME, Phipson B, Wu D, *et al.* limma powers differential expression analyses for RNA-sequencing and microarray studies. *Nucleic Acids Res* 2015; **43**: e47.
30. Peters TJ, Buckley MJ, Statham AL, *et al.* De novo identification of differentially methylated regions in the human genome. *Epigenetics Chromatin* 2015; **8**: 6.
31. Quinlan AR, Hall IM. BEDTools: a flexible suite of utilities for comparing genomic features. *Bioinformatics* 2010; **26**: 841-842.
32. McLean CY, Bristor D, Hiller M, *et al.* GREAT improves functional interpretation of cis-regulatory regions. *Nat Biotechnol* 2010; **28**: 495-501.
33. Anders S, Huber W. Differential expression analysis for sequence count data. *Genome Biol* 2010; **11**: R106.
34. Iqbal MM, Serralha M, Kaur P, Martino D. Mapping the landscape of chromatin dynamics during naïve CD4+ T-cell activation. *Sci Rep* 2021; **11**: 14101.
35. Li H, Durbin R. Fast and accurate short read alignment with Burrows-Wheeler transform. *Bioinformatics* 2009; **25**: 1754-1760.
36. Li H, Handsaker B, Wysoker A, *et al.* The Sequence Alignment/Map format and SAMtools. *Bioinformatics* 2009; **25**: 2078-2079.
37. Zhang Y, Liu T, Meyer CA, *et al.* Model-based analysis of ChIP-Seq (MACS). *Genome Biol* 2008; **9**: R137.
38. Ramírez F, Ryan DP, Grüning B, *et al.* deepTools2: a next generation web server for deep-sequencing data analysis. *Nucleic Acids Res* 2016; **44**: W160-165.
39. Love MI, Huber W, Anders S. Moderated estimation of fold change and dispersion for RNA-seq data with DESeq2. *Genome Biol* 2014; **15**: 550.
40. Cano-Gamez E, Soskic B, Roumeliotis TI, *et al.* Single-cell transcriptomics identifies an effectorness gradient shaping the response of CD4+ T cells to cytokines. *Nature Communications* 2020; **11**: 1801.

41. Butler A, Hoffman P, Smibert P, Papalexi E, Satija R. Integrating single-cell transcriptomic data across different conditions, technologies, and species. *Nature Biotechnology* 2018; **36**: 411-420.
42. Newman AM, Steen CB, Liu CL, *et al.* Determining cell type abundance and expression from bulk tissues with digital cytometry. *Nature Biotechnology* 2019; **37**: 773-782.
43. Langie SAS, Moisse M, Szarc vel Szic K, *et al.* GLI2 promoter hypermethylation in saliva of children with a respiratory allergy. *Clinical Epigenetics* 2018; **10**: 50.
44. Puck A, Aigner R, Modak M, Cejka P, Blaas D, Stöckl J. Expression and regulation of Schlafen (SLFN) family members in primary human monocytes, monocyte-derived dendritic cells and T cells. *Results Immunol* 2015; **5**: 23-32.
45. Puck A, Hopf S, Modak M, *et al.* The soluble cytoplasmic tail of CD45 (ct-CD45) in human plasma contributes to keep T cells in a quiescent state. *Eur J Immunol* 2017; **47**: 193-205.
46. Rhead B, Brorson IS, Berge T, *et al.* Increased DNA methylation of SLFN12 in CD4+ and CD8+ T cells from multiple sclerosis patients. *PLoS One* 2018; **13**: e0206511.
47. Chen MH, Liu PC, Chang CW, *et al.* Decoy receptor 3 suppresses B cell functions and has a negative correlation with disease activity in rheumatoid arthritis. *Clin Exp Rheumatol* 2014; **32**: 715-723.
48. Wu N-L, Huang D-Y, Hsieh S-L, Hsiao C-H, Lee T-A, Lin W-W. EGFR-driven up-regulation of decoy receptor 3 in keratinocytes contributes to the pathogenesis of psoriasis. *Biochimica et Biophysica Acta (BBA) - Molecular Basis of Disease* 2013; **1832**: 1538-1548.
49. Lin W-W, Hsieh S-L. Decoy receptor 3: A pleiotropic immunomodulator and biomarker for inflammatory diseases, autoimmune diseases and cancer. *Biochemical Pharmacology* 2011; **81**: 838-847.
50. Bamias G, Evangelou K, Vergou T, *et al.* Upregulation and nuclear localization of TNF-like cytokine 1A (TL1A) and its receptors DR3 and DcR3 in psoriatic skin lesions. *Exp Dermatol* 2011; **20**: 725-731.
51. Lee CS, Hu CY, Tsai HF, *et al.* Elevated serum decoy receptor 3 with enhanced T cell activation in systemic lupus erythematosus. *Clin Exp Immunol* 2008; **151**: 383-390.
52. Hsu TL, Wu YY, Chang YC, *et al.* Attenuation of Th1 response in decoy receptor 3 transgenic mice. *J Immunol* 2005; **175**: 5135-5145.
53. Chen CC, Yang YH, Lin YT, Hsieh SL, Chiang BL. Soluble decoy receptor 3: increased levels in atopic patients. *J Allergy Clin Immunol* 2004; **114**: 195-197.
54. Hsieh S-L, Lin W-W. Decoy receptor 3: an endogenous immunomodulator in cancer growth and inflammatory reactions. *Journal of Biomedical Science* 2017; **24**: 39.
55. Mueller AM, Pedré X, Killian S, David M, Steinbrecher A. The Decoy Receptor 3 (DcR3, TNFRSF6B) suppresses Th17 immune responses and is abundant in human cerebrospinal fluid. *J Neuroimmunol* 2009; **209**: 57-64.
56. Chen SJ, Wang YL, Kao JH, *et al.* Decoy receptor 3 ameliorates experimental autoimmune encephalomyelitis by directly counteracting local inflammation and downregulating Th17 cells. *Mol Immunol* 2009; **47**: 567-574.
57. Chen MH, Kan HT, Liu CY, *et al.* Serum decoy receptor 3 is a biomarker for disease severity in nonatopic asthma patients. *J Formos Med Assoc* 2017; **116**: 49-56.
58. Zhou X, Han X, Lyu SC, *et al.* Targeted DNA methylation profiling reveals epigenetic signatures in peanut allergy. *JCI Insight* 2021; **6**.
59. Do AN, Watson CT, Cohain AT, *et al.* Dual transcriptomic and epigenomic study of reaction severity in peanut allergic children. *J Allergy Clin Immunol* 2019.

60. Abdel-Gadir A, Schneider L, Casini A*, et al.* Oral immunotherapy with omalizumab reverses the Th2 cell-like programme of regulatory T cells and restores their function. *Clin Exp Allergy* 2018; **48**: 825-836.
61. Gonzales-van Horn SR, Farrar JD. Interferon at the crossroads of allergy and viral infections. *J Leukoc Biol* 2015; **98**: 185-194.
62. André F, Pène J, André C. Interleukin-4 and interferon-gamma production by peripheral blood mononuclear cells from food-allergic patients. *Allergy* 1996; **51**: 350-355.
63. Blasius AL, Giurisato E, Cella M, Schreiber RD, Shaw AS, Colonna M. Bone marrow stromal cell antigen 2 is a specific marker of type I IFN-producing cells in the naive mouse, but a promiscuous cell surface antigen following IFN stimulation. *J Immunol* 2006; **177**: 3260-3265.
64. Wolk K, Witte K, Witte E*, et al.* IL-29 is produced by T(H)17 cells and mediates the cutaneous antiviral competence in psoriasis. *Sci Transl Med* 2013; **5**: 204ra129.
65. Ohshima M, Kanda H, Kubo K, Yonezumi-Hayashi A, Tateishi S, Yamamoto K. Characterization of 5C11-positive activated interferon-producing cells in patients with systemic lupus erythematosus. *Lupus* 2013; **22**: 44-51.
66. Herbert C, Shadie AM, Bunting MM*, et al.* Anti-inflammatory and anti-remodelling effects of ISU201, a modified form of the extracellular domain of human BST2, in experimental models of asthma: association with inhibition of histone acetylation. *PLoS One* 2014; **9**: e90436.
67. Huber JP, Gonzales-van Horn SR, Roybal KT, Gill MA, Farrar JD. IFN-α suppresses GATA3 transcription from a distal exon and promotes H3K27 trimethylation of the CNS-1 enhancer in human Th2 cells. *J Immunol* 2014; **192**: 5687-5694.
68. Huber JP, Ramos HJ, Gill MA, Farrar JD. Cutting edge: Type I IFN reverses human Th2 commitment and stability by suppressing GATA3. *J Immunol* 2010; **185**: 813-817.

Figure Legends

Figure 1: (a) Outline of study; naive CD4 T cells ($CD4^+$,$CD45RA^+$, $CCR7^+$) from 18 non-food allergic adolescents (NA) and 29 food allergic adolescents (FA) were isolated using fluorescence activated cell sorting, and then cultured for 72 hours with RPMI alone (baseline) or in RPMI+anti-CD3/anti-CD28 beads. DNA was collected from cells at baseline and stimulated conditions, while RNA was collected from the stimulated cells. **(b)** Key comparisons carried out and summary of differentially methylated probes (DMPs) and differentially methylated regions (DMRs) arising from each comparison. *Differentially methylated probes (DMPs), unadjusted P-value <0.01, $\Delta\beta$ >5%. ‡ Differentially methylated probes (DMPs), adjusted P-value <0.01, $\Delta\beta$ >5%. † Differentially methylated regions (DMRs), unadjusted P-value <0.05, >3 probes in DMR, at least one probe showing $\Delta\beta$ >5%

Figure 2: (a) Principal components analysis (PCA) of total DMPs from comparisons of quiescent vs activated NA and FA samples, indicating clear separation of quiescent and activated samples, but not NA and FA groups. Circles represent quiescent samples, while triangles represent activated samples. Red denotes NA samples, while turquoise denotes FA samples. **(b)** Venn diagram of significantly activated probes activated across NA and FA groups (adjusted P-value <0.01, $\Delta\beta$ >5% between activated and quiescent samples).

Figure 3: (a) Volcano plot of significant (P value <0.01) differentially methylated probes (DMPs) in quiescent NAvFA comparison, (-log10 p value on y axis, methylation difference on x-axis), with probes reaching $\Delta\beta$ threshold (5%) shown in red. **(b)** PCA plot of 347 probes separating NA and FA samples (NA in red, FA in turquoise). **(c)** Boxplots of methylation values of selected probes from NA vs FA comparison showing distinct differences between NA and FA samples at baseline. Values displayed above boxplots represent *P* values determined by the Mann–Whitney U-test between groups. **(d)** Dendrogram of hierarchical clustering (determined using Euclidean distance between samples) of samples based on 347 DMPs from the quiescent comparison, **(i)** across quiescent samples, and **(ii)** across activated samples.

Figure 4: (a) Volcano plot of significant (*P* value <0.01) differentially methylated probes (DMPs) in activated NAvFA comparison, (-log10 p value on y axis, methylation difference on x-axis), with probes reaching $\Delta\beta$ threshold (5%) highlighted in yellow**. (b)** PCA of all 594 DMPs across all samples, showing separation of NA and FA samples, in addition to activated and quiescent samples. **(c)** Dendrogram of hierarchical clustering of samples based on 289

DMPs from the activated comparison, **(i)** across quiescent samples, and **(ii)** across activated samples. **(e)** Boxplots of probes linked to genes associated with Th1/Th2 differentiation in quiescent and activated FA samples. Values displayed above boxplots represent *P* values determined by the Mann–Whitney U-test between groups

Figure 5: (a) Workflow employed to carry out CD4T cell deconvolution analysis. Signature matrix construction and cell fraction imputation was carried out using the CIBERSORTx tool. **(b)** Boxplots of cell fraction imputations for cell types with significantly different expression signatures--IFN-producing cell signatures and iTreg cell signatures. **(c)** Heatmap of 89 differentially expressed genes (*P* value <0.05, FC > 1.5) between activated NA and FA samples. **(d)** PCA plot showing separation of NA and FA samples based on these 89 DEGs**. (e)** Results of functional enrichment analysis (GO: biological process) of these 89 DEGs, showing enrichment for a number of interferon-associated pathways. Terms associated with viral/interferon responses are highlighted in red.

Figure 6: (a) Diagram of type 1 interferon and interferon gamma signalling pathway, highlighting genes showing differential gene expression, cytokine concentration, and methylation in activated FA samples. **(b)** Boxplots comparing cytokine concentration (normalized log2 pg/ml) and gene expression (normalized log2RPKM values) of *IFNG* in activated NA and FA samples**.(c)** Boxplots of methylation values (scaled) of significant DMPs in *BST2* DMR between stimulated NA and FA groups. **(d)** Location of the *BST2* DMR relative to *BST2* gene**. (i)** Location of DMR probes on the chr19 chromosome (p arm) and proximity to nearest gene, *BST2*. **(ii)** Overlaid with ATAC-seq data from quiescent and activated healthy naïve CD4T cells indicate regions of open chromatin **(iii)** Mean methylation values (β values) of probes in NA and FA groups within DMR. Significance of DMR was identified using DMRCate, which uses the moderated t-statistic of each probe within the specified comparison (NA vs FA), to model smoothed test statistics using the Satterthwaite approach. Error bars represent 95% confidence intervals.

Description of supplementary materials:

Supplementary Figure 1: (a) Heatmap of contribution of each trait to principal components (PCs). The value at the top signifies the correlation coefficient, while the value in the brackets is the p-value of each trait for the first 20 PCs. Traits that showed an R2 >0.2 and p <0.05 were

identified as contributing significantly to a PC and are highlighted as blue (negative correlation) and red (positive correlation). **(b)** Plot of first 10 principal components and their contribution to variation of samples. **(c)** Boxplots of the $\Delta\beta$ values (quiescent vs activated) of the NA-specific (1,081 DMPs), commonly activated probes (6,595 DMPs), and FA-specific probes (3,908 DMPs) across NA and FA samples. Values displayed above boxplots represent *P* values determined by the Mann–Whitney U-test between groups. **(d)** Boxplots of fold-change of ATAC-peak reads at the NA-specific probes, commonly activated probes, and FA-specific probes across NA and FA samples, separated into groups of probes showing loss of methylation following activation, and those showing a gain in methylation following activation. Values displayed above boxplots represent *P* values determined by the Mann–Whitney U-test between groups.

Supplementary Figure 2: (a) Distribution of probe sets relative to CpG islands. **(b)** Distribution of ATAC peaks across probe sets, separated into probes showing gain in methylation following activation, and probes showing loss in methylation following activation. **(c)** Results of functional enrichment analysis carried out on each probe set.

Supplementary Figure 3: (a) Distribution of ATAC peaks across NAvFA DMPs at quiescence, separated into probes showing higher methylation in FA samples, and probes showing lower methylation in FA samples.**(b)** Distribution of ATAC peaks across NAvFA DMRs at quiescence, separated as in (a). **(c)(i)** Distribution of quiescent NAvFA DMPs relative to CpG islands. **(ii)** Distribution of quiescent NAvFA DMRs relative to CpG islands. **(d)** Scatterplot showing distribution of DMRs in comparison, number of probes in DMR (y-axis) plotted against size of DMR (in bp). Points are coloured based on direction of methylation in FA samples (blue-higher methylation in FA, grey- lower methylation in FA). **(e)** Location of the *TNFRSF6B* DMR relative to *TNFRSF6B* gene. (i) Location of DMR probes on the chr20 chromosome (p arm) and proximity to nearest gene, *TNFRSF6B*. Overlaid with ATAC-seq data from quiescent and activated non-food allergic naïve CD4T cells indicate regions of open chromatin. **(ii)** Mean methylation values (β values) of probes in NA and FA groups within DMR. Error bars represent 95% confidence intervals.

Supplementary Figure 4: (**a)** Distribution of ATAC peaks across NAvFA DMPs following activation, separated into probes showing higher methylation in FA samples, and probes showing lower methylation in FA samples. **(b)** Distribution of ATAC peaks across NAvFA DMRs following activation, separated as in (a). **(c)(i)** Distribution of activated NAvFA DMPs

relative to CpG islands. **(ii)** Distribution of quiescent NAvFA DMRs relative to CpG islands. **(d)** Principal components analysis (PCA) of total DMPs from comparison of activated NA and FA samples, indicating clear separation of activated NA and FA samples. **(e)** Scatterplot showing distribution of DMRs in activated NAvFA comparison, number of probes in DMR (y-axis) plotted against size of DMR (in bp). Points are coloured based on direction of methylation in FA samples (green-higher methylation in FA, orange- lower methylation in FA). (f) Boxplot showing expression of *BST2* in NA and FA samples.

Supplementary Figure 5: (a) Heatmap showing results of cell fractionation analysis using CIBERsortx. **(b)** Boxplots showing results of fractionation analysis (scaled enrichment values) for expression signatures of Th0, Th17, Th2, HSP (heat shock protein/cellular stress-marker expressing) CD4 T cell subsets.

Supplementary Table 1: List of all DMPs from quiescent vs activated comparisons in NA and FA.

Supplementary Table 2: Top KEGG terms from functional enrichment analysis of commonly activated, NA-specific and FA-specific probes from quiescent vs activated comparisons.

Supplementary Table 3: List of DMPs from NA vs FA comparisons in quiescent and activated samples.

Supplementary Table 4: List of DMRs from NA vs FA comparisons in quiescent and activated samples.

Supplementary Table 5: Top KEGG terms from functional enrichment analysis of DMPs from comparison of activated NA vs FA samples.

Supplementary Table 6: List of DEGs from NA vs FA comparison in activated samples.

Supplementary Table 7: Top GO terms from functional enrichment analysis of DEGs from comparison of activated NA vs FA samples.

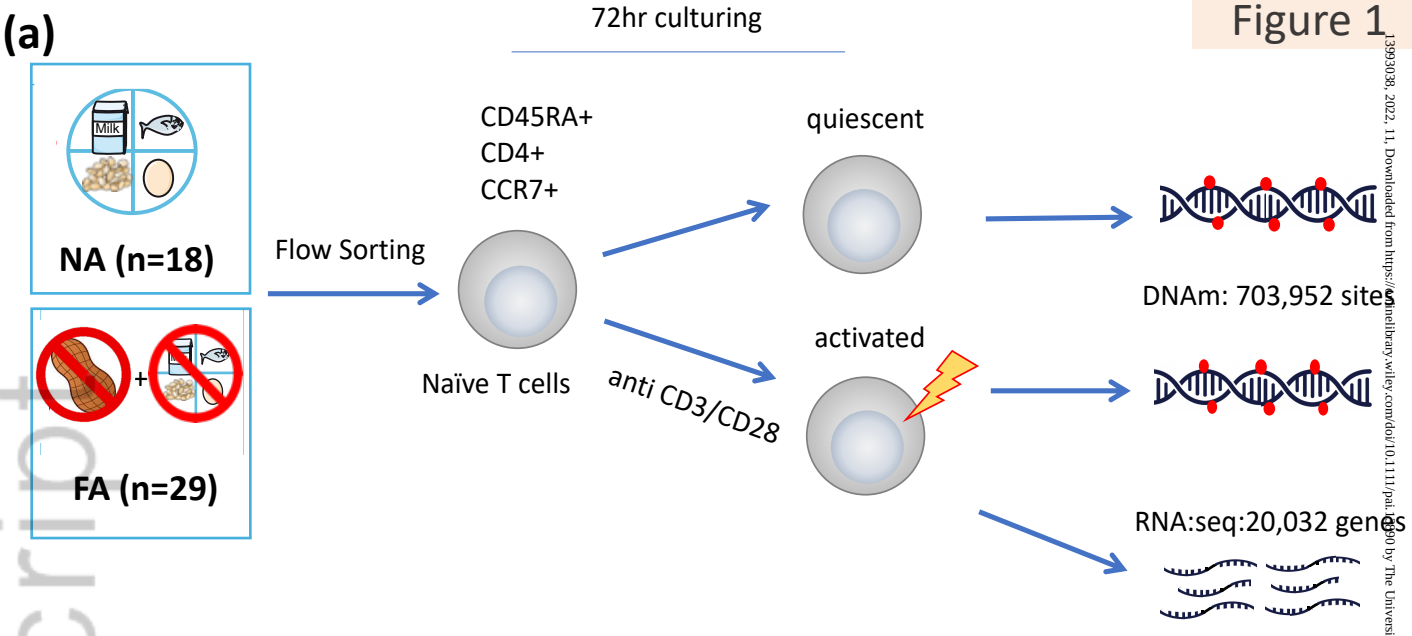

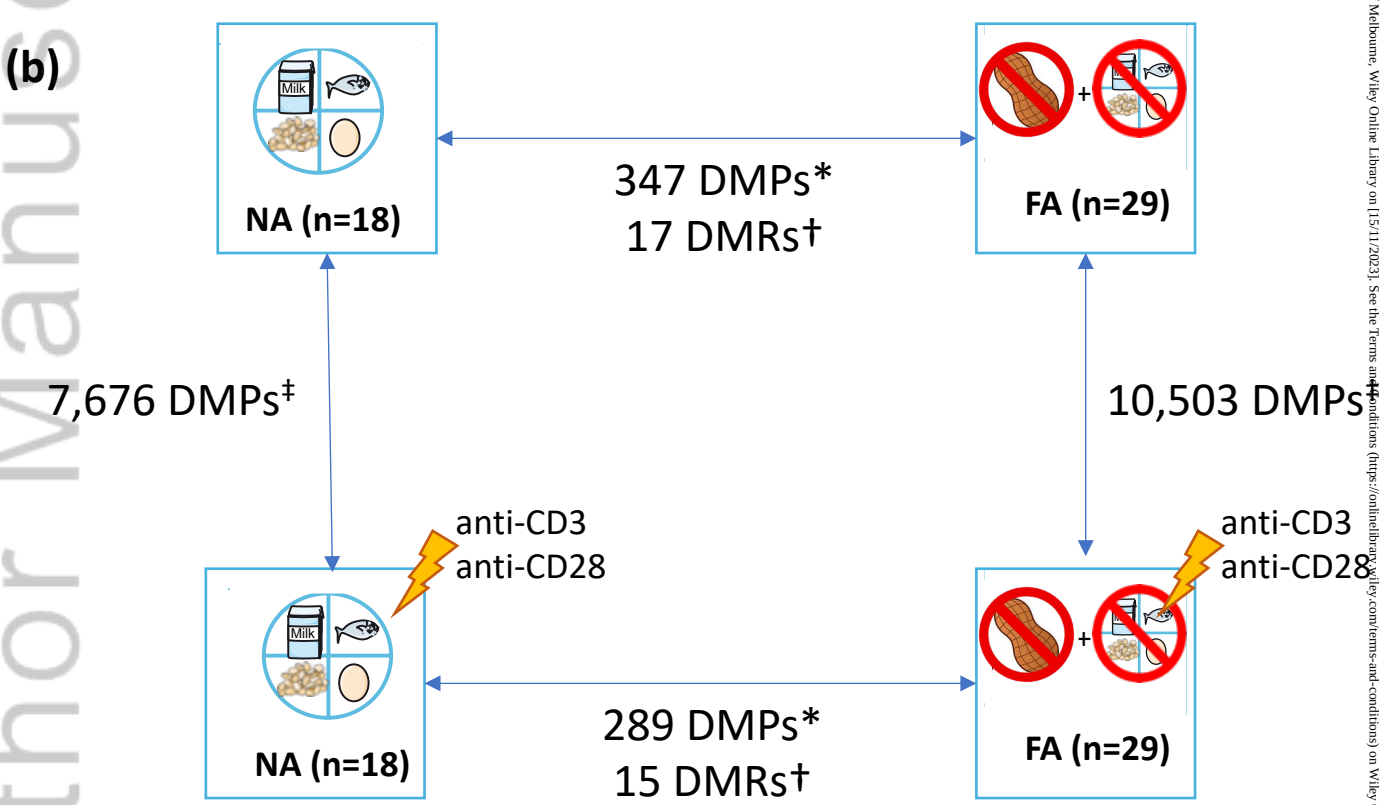

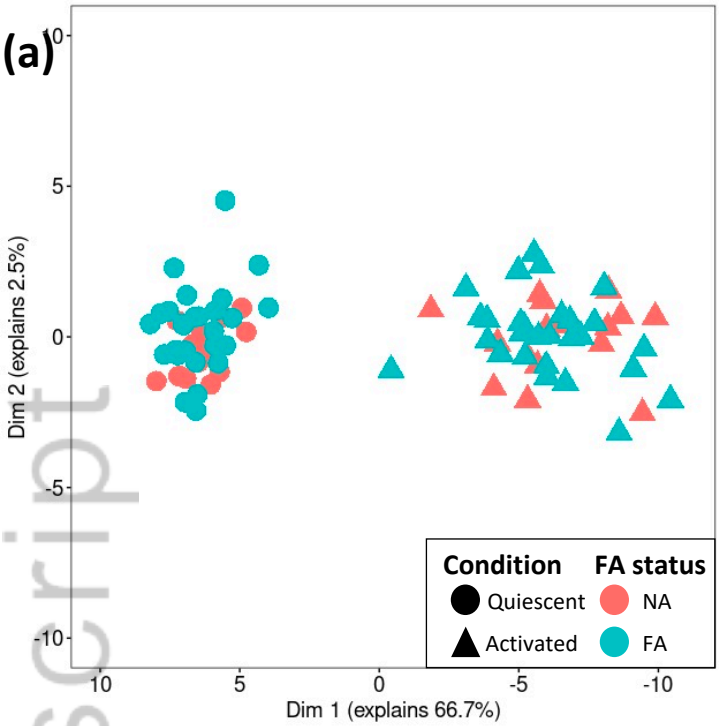

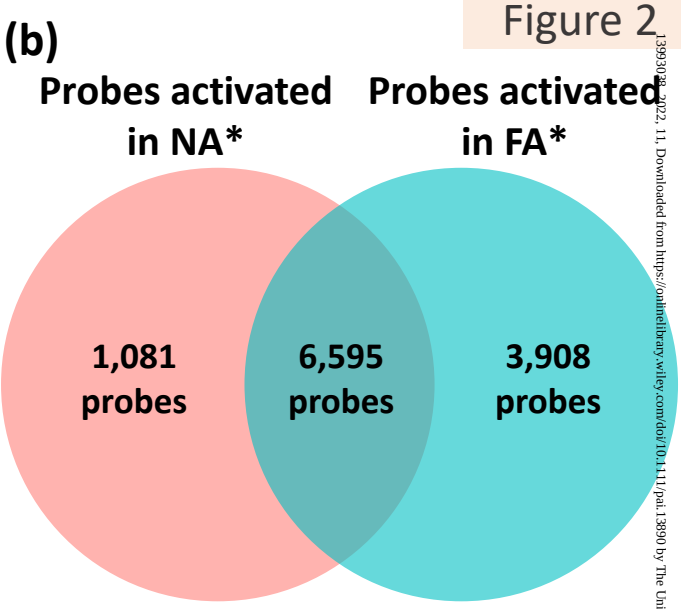

Figure 3

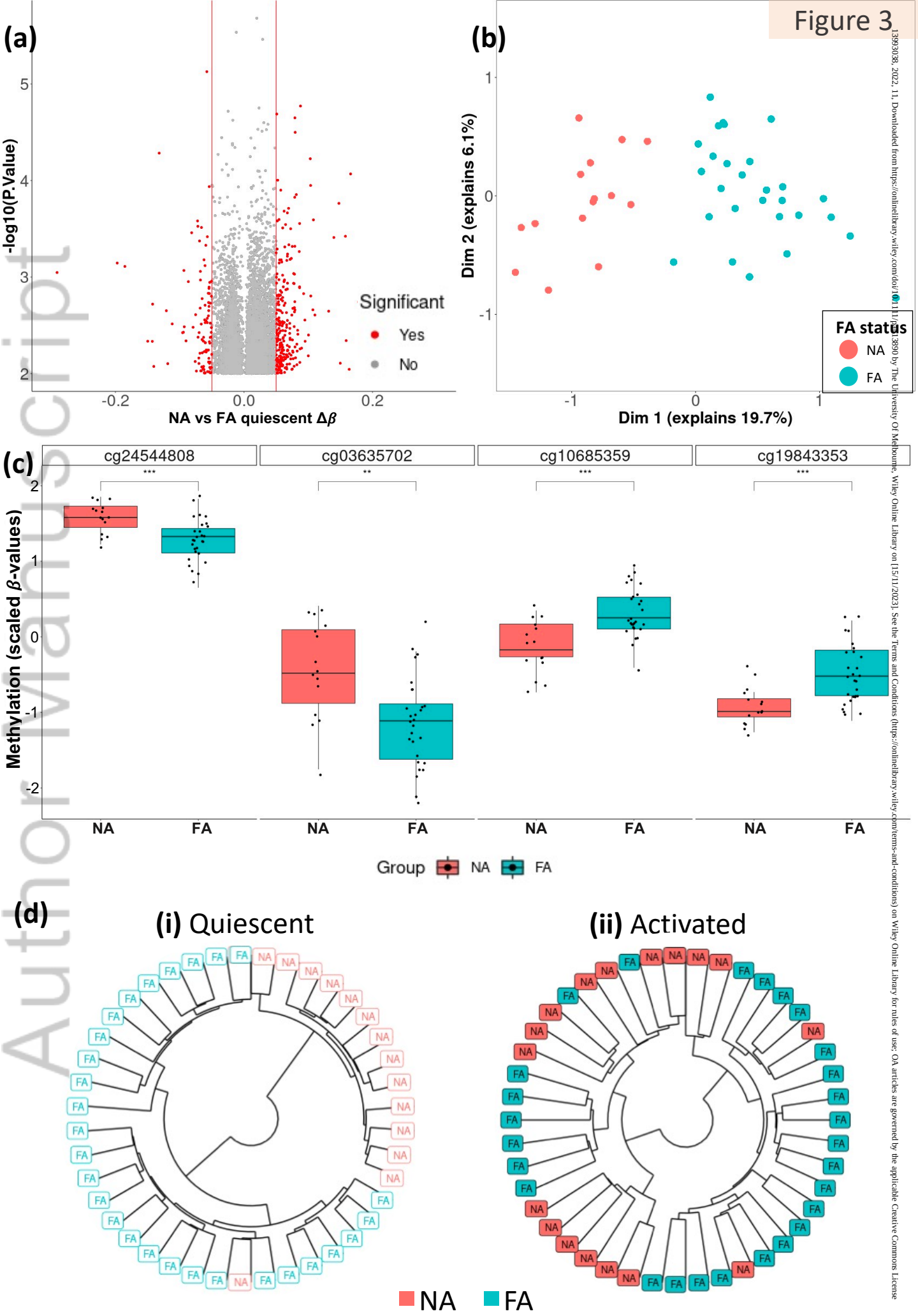

Figure 4